Laboratori Nazionali di Frascati

LNF-71/94

B. Bartoli, F. Felicetti, H. Ogren, V. Silvestrini, G. Marini, A. Nigro, N. Spinelli and F. Vanoli : HIGH-ENERGY ELECTRON-POSITRON ELASTIC SCATTERING

Estratto da : Phys. Letters 36B, 593 (1971)

HIGH-ENERGY ELECTRON-POSITRON ELASTIC SCATTERING

B. BARTOLI, F. FELICETTI, H. OGREN and V. SILVESTRINI
Laboratori Nazionali di Frascati del CNEN, Frascati, Italy

G. MARINI, A. NIGRO and N. SPINELLI
Istituto di Fisica dell'Università, and Sezione di Roma dell'INFN, Rome, Italy

and

F. VANOLI
Istituto di Fisica Superiore dell'Università, and Sezione di Napoli dell'INFN, Naples, Italy

Received 20 August 1971

We present the analysis of 5164 wide angle Bhabha events collected at several c.m. energies between 1.4 and 2.4 GeV using the Frascati $e^+ - e^-$ storage ring, ADONE. The results are in agreement with the predictions of quantum electrodynamics within the experimental errors (±10%).

Measurements of wide angle high energy (1.4 - 2.4 GeV total c.m. energy) electron-positron elastic scattering have been performed at ADONE, the Frascati 2×1.5 GeV e^+e^- storage ring. Some preliminary results (in the c.m. energy between 1.6 and 2.0 GeV) have already presented elsewhere [1].

The experimental apparatus, shown in fig. 1, surrounds one of the straight sections of ADONE,

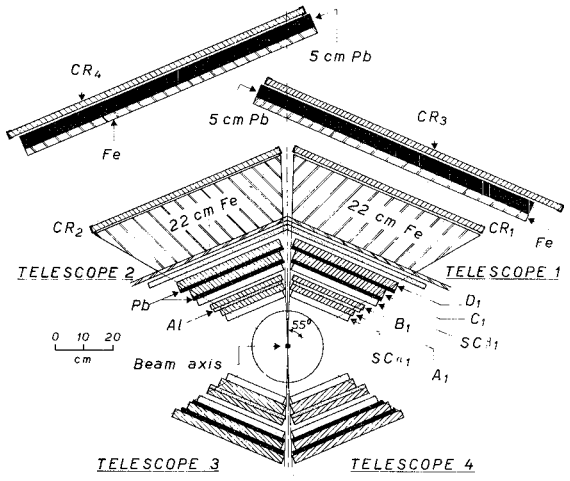

Fig. 1. Section of the experimental apparatus orthogonal to the beam axis. The θ acceptance is between 60° and 120° (z-axis being along the beam direction).

and covers about 0.35 of the total solid angle, as seen from the center of the apparatus.

Each of the four telescopes T_i consists of two magnetostrictive monogap wire spark chambers, SC α and SC β, which measure the azimuthal direction, φ, of the particle (z-axis being along the beam direction) and of four scintillation counters $A_iB_iC_i$ and D_i. There is 1.3 cm of Al between the counters A_i and B_i, while two 0.7 cm Pb absorbers are placed in front of each of the counters C_i and D_i, forming a sandwich that is used for pulse height analysis to discriminate showering electrons from minimum ionizing particles (mainly cosmic rays, C.R.). A thick absorber (22 cm of Fe), covering the top telescopes, and the roof counters CR_1, CR_2, in anticoincidence with our trigger, strongly suppress the detected cosmic ray flux. Counters CR_3 and CR_4 were added in a second set of measurements and will be discussed later.

A charged particle in telescope T_i is defined by the coincidence $T_i \equiv A_i B_i (C_i + D_i)$ and a neutral particle by $N_i \equiv (\bar{A}_i + \bar{B}_i)(C_i + D_i)$. Any coincidence of two (or more) charged particles, T_i, each in a different telescope, defines the master trigger, $CR \equiv (CR_1 + CR_2)$ being in anticoincidence*.

* To give a coincidence, an electron must traverse 24 g/cm^2 of absorber, corresponding to ~ 1.9 radiation length, x_0; to be vetoed by CR_1, CR_2, it must traverse $15x_0 = 203$ g/cm^2; to reach CR_3, CR_4 it must traverse $25.2\, x_0 = 282$ g/cm^2.

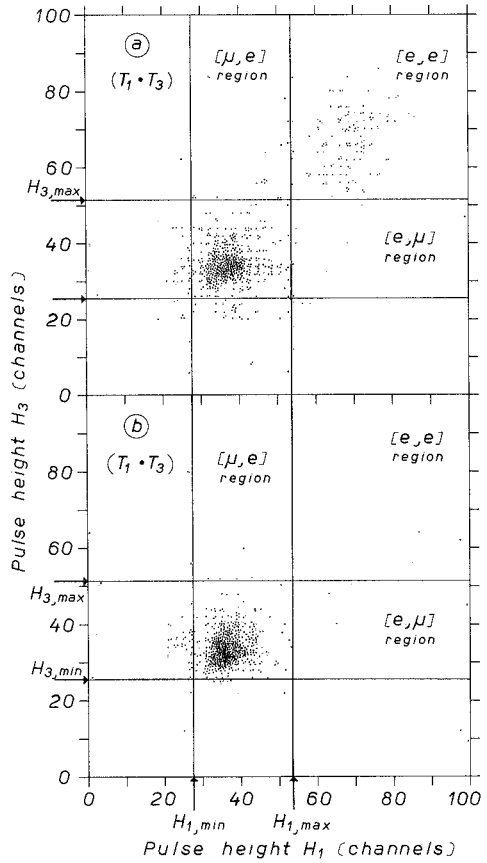

Fig. 2. Plot of pulse heights H_3 versus H_1 for $(T_1 \cdot T_3)$ events. (a) in-time events. (b) out-of-time events.

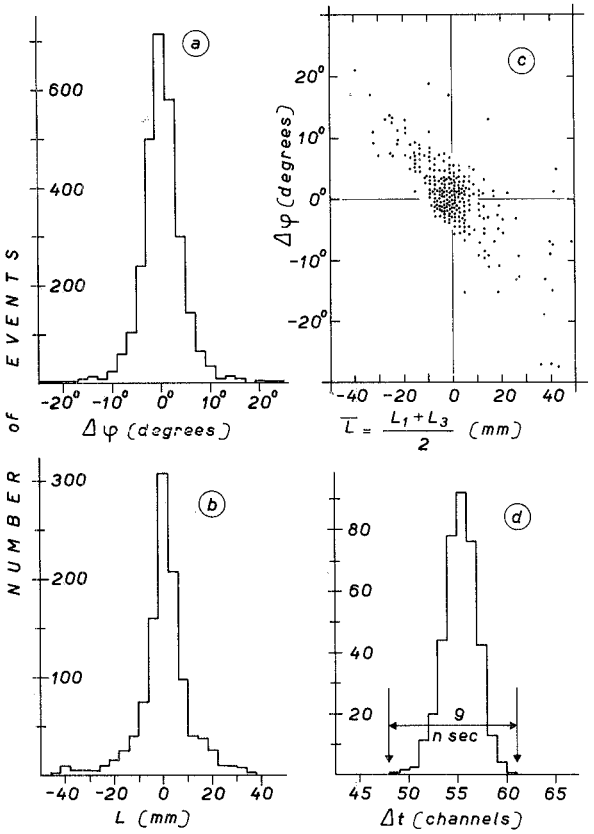

Fig. 3. Track analysis of a sample of [e,e] events. (a) $\Delta\varphi$ distribution for in-time events. (b) $\bar{L}$ distribution for in-time events. (c) $\Delta\varphi$ versus $\bar{L}$ correlation for in-time events. (d) Δt distribution for events from the source.

When a master trigger occurs a PDP8 computer records: which coincidences T_i were involved in the event; the azimuthal coordinates of the tracks in the spark chambers, with the restriction that when there is more than one track in a chamber, only that closest to the magnetostrictive pickup is recorded; the pulse height, H_i, in counters $(C_i + D_i)$ for each telescope; the time, Δt, of the event with respect to the beam-beam impact*.

Date reduction. The first step in the analysis is to display the events which give a coincidence between opposite telescopes $(T_1 \cdot T_3)$, and $(T_2 \cdot T_4)$, as a function of Δt. Their distribution shows a very clear peak (±2 nsec h.w.h.m.) superimposed on a smooth background of cosmic rays. This allows us to define an interval of Δt for events *in-time* with the beam-beam interaction.

Fig. 2(a) shows a typical pulse height plot of H_3 versus H_1 for in-time $(T_1 \cdot T_3)$ events. The plot contains two heavily populated regions: a low pulse height region of minimum ionizing particles (C.R.) and a large pulse height region of events with both particles producing a detectable shower, which we designate as the [e,e] region. Out-of-time events (fig. 2(b)) show only the cluster in the minimum ionizing region, while the [e,e] region is practically empty. Track reconstruction using the wire spark chambers allows us to conclude that all but a small fraction of the [e,e] events are Bhabha scattering events.

Fig. 3 shows the track analysis of a sample of in-time [e,e] events. In fig. 3(a) the [e,e] events clearly appear to be coplanar (i.e. $\Delta\varphi = 0$, where $\Delta\varphi$ is the angle between the two planes parallel to the beam axis containing the two

* In ADONE there are three bunches of e^+ and three bunches of e^-, each of duration ~ 1-2 nsec (f.w.h.m.). They collide in the experimental sections every ~100 nsec.

tracks). The $\pm 3^{\circ}$ angular spread (h.w.h.m.) is due to spark chamber resolution and multiple scattering in the vacuum chamber walls (0.15 cm of Fe) and in the telescope absorbers. The [e,e] events in fig. 3(b) are plotted as a function of the distance, L, between the track and the axis of the beam. Almost all of the events appear to originate, within a h.w.h.m. ± 5 mm, of the beam region. Also in this case multiple scattering and spark chamber resolution account for the observed width (the actual beam dimensions are $\sim 1\times 1$ mm^2). This interpretation of the experimental widths of the $\Delta\varphi$ and L distributions is confirmed in fig. 3(c). The clear correlation observed between $\Delta\varphi$ and the average distance ($\bar{L}$) of the two particles from the beam is what one would expect if all of the events originate with $\Delta\varphi = 0$ in the $\sim (1\times 1)$mm^2 source region. Finally fig. 3(d) shows how well we can define the region of the [e,e] events which are "in-time" with the beam-beam impact. Furthermore the out-of-time contamination (mainly C.R.) appears to be negligible.

From this analysis we can conclude that (apart from small background subtractions hereafter discussed) the [e,e] events are two body events with charged showering particles originating in e^+e^- collisions, i.e. they are Bhabha elastic scattering events.

A reliable track analysis of the data requires that all the four chambers involved in the event have correctly fired. Since the efficiency of each chamber has been measured to be about 0.85 - - 0.95, we have considerably fewer "4 chamber electron events" than we have [e,e] events. However we conclude from the above track analysis that, for evaluation of the cross-section, we can use all the detected [e,e] events, i.e. those that satisfy the mentioned pulse height requirements, irrespective of spark chamber information. In this way we avoid any problems due to the spark chambers inefficiency.

During 1341 hours of running time, with an integrated luminosity $\mathcal{L} \simeq 3.5\times 10^{35}$ cm^{-2}, we have collected a total of 5164 [e,e] events in a range of c.m. energies, $E_+ + E_-$, between 1.4 and 2.4 GeV. They are listed, at each c.m. energy, in column (3) of table 1.

Two different types of background are to be subtracted from these numbers:

i) a C.R. background which can be easily evaluated experimentally from the number of out-of-time [e,e] events. This subtraction is of the order of $\sim 2\%$ (see column (4) table 1);

ii) a contamination due to interactions of either beam with the residual gas in the storage ring. With measurements performed with only a

Table 1.
List of the experimental results and of the background corrections. The numbers marked with a * refer to runs in which the counters CR_3, CR_4 were put in anticoincidence with the trigger.

C.m. energy $E_+ + E_-$ (GeV)	Integrated luminosity (cm^{-2})	Collected [e,e] events	Normalized C.R. background	Normalized beam-gas background	Corrected e^+e^- Bhabha events	m Small-angle monitor events	$R = \frac{e^-e^+}{m} \times 10^3$	q^2 (GeV/c)^2
(1)	(2)	(3)	(4)	(5)	(6)	(7)	(8)	(9)
1.4	68×10^{32}	212	3.9 ± 1.2	0.2 ± 0.7	761 ± 45	198.4×10^3	3.83 ± 0.22	0.87
1.4	113×10^{32}	306*	5.3 ± 1.2	-0.6 ± 0.9				
1.5	52×10^{32}	141	3.6 ± 1.1	0.2 ± 0.8	1098 ± 45	308.9×10^3	3.56 ± 0.15	0.95
1.5	280×10^{32}	738*	13.6 ± 1.9	-1.6 ± 2.4				
1.6	77×10^{32}	176	4.5 ± 1.2	1.1 ± 1.2	222 ± 21	64.6×10^3	3.44 ± 0.32	1.08
1.65	114×10^{32}	187	3.8 ± 1.1	2.1 ± 1.8	230 ± 20	87.6×10^3	2.62 ± 0.23	1.14
1.7	126×10^{32}	259	3.8 ± 1.1	3.2 ± 2.2	332 ± 25	89.8×10^3	3.70 ± 0.28	1.21
1.75	135×10^{32}	192	4.2 ± 1.2	3.7 ± 2.3	238 ± 22	88.3×10^3	2.70 ± 0.25	1.29
1.8	135×10^{32}	226	3.1 ± 1.0	4.8 ± 2.6	283 ± 24	81.3×10^3	3.48 ± 0.29	1.36
1.85	260×10^{32}	417	7.7 ± 1.6	2.6 ± 2.3	1470 ± 56	377.4×10^3	3.68 ± 0.14	1.44
1.85	420×10^{32}	825*	7.2 ± 1.5	5.6 ± 10.0				
1.9	134×10^{32}	186	4.2 ± 1.2	8.6 ± 3.2	220 ± 20	68.3×10^3	3.22 ± 0.30	1.52
2.0	290×10^{32}	328	7.6 ± 1.6	30.2 ± 6.0	369 ± 30	128.2×10^3	2.88 ± 0.23	1.68
2.4	148×10^{32}	102	3.6 ± 1.1	4.0 ± 2.7	1045 ± 52	303.2×10^3	3.45 ± 0.17	2.42
2.4	1147×10^{32}	869*	15.1 ± 2.1	69.5 ± 17.9				
Totals	3499×10^{32}	5164	91.2 ± 5.3	133.6 ± 22.5	6268 ± 117	1795.9×10^3		

single beam or with two separated beams † we have determined that the contamination is near zero at low energy, but rises to ~ 8% at 2.4 GeV c.m. energy. The average contamination for the full sample is about 2% (see column (5) of table 1).

After background subtractions are performed, we are left with 4939 [e,e] elastic scattering events. In order to obtain the total number of produced Bhabha events we have to apply to our data several corrections.

First, since the probability that an electron will initiate a shower before counter C and D is not 100%, we expect that a small fraction of events $e^+e^- \to e^+e^-$ will not appear in the [e,e] region. To evaluate the size of this "shower-correction" we have analyzed the events which fall in the [μ,e] region of fig. 2 (i.e. the events with only one pulse height larger than $H_{i,\max}$). As we expect if these [μ,e] events are true e^+e^- scattering events, we find that their L and $\Delta\varphi$ distributions appear to be the same as for the [e,e] events. After background subtractions are performed, from the number of [μ,e] events we are able to determine the probability, ϵ, for an electron to have a pulse height less than $H_{i,\max}$. This has been done at each energy, and the correction factors $F_S = (1-\epsilon)^{-2}$ to be applied to the [e,e] events are listed in column (2) table 2.

Furthermore, some events will be lost if one of the electrons passes through the 22 cm of Fe and produces an anticoincidence pulse in counters CR_1, CR_2. For this reason in a later phase of the experiment we placed over the apparatus a second "roof" of 1.5 cm of Fe, 5 cm Pb and two additional counters CR_3, CR_4 (see fig. 1). These counters were put in anticoincidence with the trigger, while CR_1, CR_2 were simply recorded for each event. In this way we directly measured the fraction of e^+e^- events that were lost due to anticoincidence in CR_1 and CR_2. The correction factors, F_{AC}, experimentally obtained are listed in column (3) of table 2. They apply only to the runs with CR_1, CR_2 in anticoincidence, since the number of events vetoed by CR_3, CR_4 was determined to be negligible. This correction has a linear energy dependence and varies from 4% at 1.4 to 15% at 2.4 GeV (see fig. 2(d) of ref.2).

Column (6) of table 1 contains the number of $e^+e^- \to e^+e^-$ events corrected for all the above mentioned effects ††.

Analysis of the results. To compare our results with QED predictions, we take the ratio, $R = e^+e^-/m$, of the wide angle Bhabha scattering events (e^+e^-) to the "monitor" events (m), namely the small angle ($3.5 \leqslant \theta \leqslant 6^\circ$ Bhabha scattering events collected simultaneously in a separate experimental apparatus [3] in a contiguous straight section of ADONE †††. This minimizes in the experimental data the energy dependence arising from the fact that the source (which is defined as the region of interaction of positron and electron bunches) has a finite energy dependent length ‡ which is comparable to the linear dimensions of our counters and which reduces the effective solid angle of the apparatus to ~ 0.18 of the total 4π str. The experimental ratios are listed in table 1, column (8) for each c.m. energy.

This ratio can be calculated from QED by integrating the Bhabha cross section over the experimental apparata in which the large angle and small angle e^+e^- scattering events were collected. For comparison with the experimental ratios we have included in the calculation of R_{th} several energy independent systematic corrections. These systematic corrections are: multiple scattering losses $(2.5 \pm 2)\%$, possible geometrical misalignement of the apparatus with respect to the beam $(3 \pm 3)\%$, and an overall uncertainty of $\pm 5\%$ in the absolute normalization of the monitor. Radiative corrections were not applied since they were calculated to be negligible ($\lesssim 1\%$).

In fig. 4 we show as a function of the c.m. total energy the experimental values of R com-

† The value of the normalization factor to be applied to the number of beam-gas events collected in the background runs has been obtained by monitoring single bremsstrahlung on the residual gas.

†† Further small corrections (like multiple scattering losses and geometrical misalignements) have not been applied to the experimental points, but, since they are calculated to be approximately constant over the whole energy range, were taken into account in the evaluation of the theoretical predictions.

††† The symmetry of the machine and the fact that the data were collected during a long period of time, averaging over possible slight changes of the working conditions of the machine, make it reasonable to assume that the overall results are not affected by the fact that small- and large-angle elastic scattering were measured in different straight sections of ADONE.

‡ The expected distribution of the source is

$$N(l) = N_0 \exp(-l^2/2l^2)$$

where l (cm) is theoretically expected to be $20E_\pm^{3/2}$ ($E_\pm$ in GeV), and experimentally has been determined as $(22 \pm 2)E_\pm^{3/2}$ (private communications of the ADONE machine staff).

Table 2.
List of the shower inefficiency correction factors F_S and of the anticoincidence-losses correction factors F_{AC}, at each total c.m. energy $E_+ + E_-$.

$E_+ + E_-$ (GeV)	F_S	F_{AC}
1.40	1.31 ± 0.07	1.046 ± 0.018
1.50	1.18 ± 0.06	1.043 ± 0.010
1.60	1.23 ± 0.06	1.060 ± 0.015
1.65	1.19 ± 0.05	1.066 ± 0.016
1.70	1.23 ± 0.05	1.072 ± 0.017
1.75	1.20 ± 0.06	1.078 ± 0.017
1.80	1.20 ± 0.05	1.082 ± 0.020
1.85	1.14 ± 0.08	1.089 ± 0.020
1.90	1.16 ± 0.05	1.094 ± 0.022
2.00	1.15 ± 0.05	1.105 ± 0.024
2.40	1.10 ± 0.08	1.153 ± 0.035

pared with the theoretical value R_{th}. Due to the systematic uncertainties mentioned above, R_{th} appears as a band with an overall width of $\sim \pm 7.5\%$. Furthermore, due to erratic changes of the beam trajectory with respect to the monitor apparatus we have added a ±5% uncertainty‡‡ (small rectangles in fig. (4)) to the statistical error of each experimental value of R. The slight energy dependence of R_{th} is due entirely to the energy dependence of the source length. Within the experimental errors the measured ratios are in agreement with the theoretical predictions.

In the Bhabha scattering around 90° the scattering diagram dominates the annihilation diagram so that our measurements are mainly characterized by the square of the four-momentum transfer to the virtual space-like photon, q^2. The values of q^2 averaged over the acceptance of our apparatus (see fig. 4) are listed in table 1 column (9) for each c.m. energy.

We can conclude that for average values of $\langle q^2 \rangle$ ranging from 0.82 $(\mathrm{GeV}/c)^2$ to 2.42 $(\mathrm{GeV}/c)^2$ the measured Bhabha cross section agrees both in slope and absolute value with the QED predictions with an overall experimental uncertainty of ~ 10%.

‡‡ We have evaluated this uncertainty by analyzing the relative variations of two symmetric telescopes of the monitor apparatus.

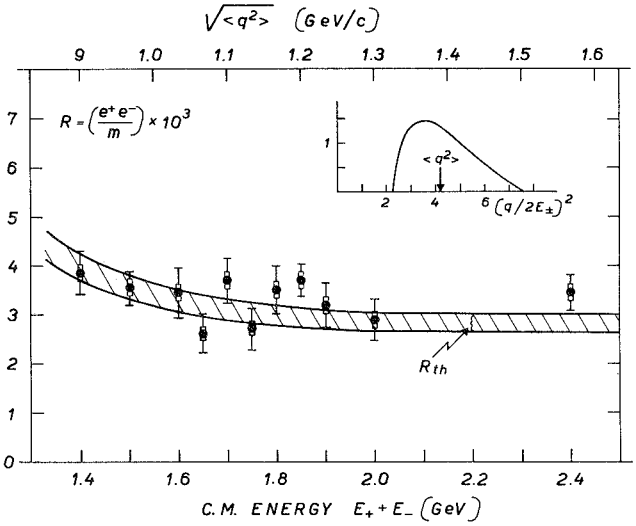

Fig. 4. The ratio R of wide angle Bhabha events (e^+e^-) to the "monitor" small angle scattering events (m) as a function of the total c.m. energy. The experimental points are compared with the R_{th} band. The q^2 acceptance of the apparatus weighted on the Bhabha cross section is shown in the upper right-band corner.

References

[1] B. Bartoli, B. Coluzzi, F. Felicetti, G. Goggi, G. Marini, F. Massa, D. Scannicchio, V. Silvestrini and F. Vanoli, Nuovo Cimento 70A (1970) 615.
[2] B. Bartoli, F. Felicetti, G. Marini, A. Nigro, H. Ogren, V. Silvestrini, N. Spinelli and F. Vanoli, Phys. Letters 36B (1971) 598.
[3] G. Barbiellini, B. Borgia, M. Conversi and R. Santonico, Rend. Classe Sci. Mat. Fis. e Nat. dell'Accad. Naz. dei Lincei 44 (1968) 44; G. Barbiellini, B. Borgia, M. Conversi, G. Iorio and R. Santonico, Intern. Report n. 155 Istituto Fisica, Università di Roma (1968).

* * * * *